Paleoceanography and Paleoclimatology

RESEARCH ARTICLE
10.1029/2024PA004873

Evolution of West-East Contrast in the Subarctic Pacific Gyre During the Plio-Pleistocene Based on Palynological Evidence at ODP Sites 882 and 887

C. Zorzi[1,2,3] **and A. de Vernal**[1]

[1]GEOTOP, Université du Québec à Montréal, Montréal, QC, Canada, [2]Centre of Marine Sciences (CCMAR/CIMAR LA), Campus de Gambelas, Universidade do Algarve, Faro, Portugal, [3]Instituto Português do Mar e da Atmosfera (IPMA), Avenida Alfredo Magalhães Ramalho 6, Lisbon, Portugal

Key Points:

- Dinocyst assemblages in the subarctic Pacific record changes in temperature and productivity through the Plio-Pleistocene
- The major transitions reflect halocline onset at 2.7 Ma and a major cooling at 1.7 Ma
- Subarctic ocean temperature and Westerlies migration may have affected northward moisture supply and ice-sheet growth over North America

Supporting Information:

Supporting Information may be found in the online version of this article.

Correspondence to:

C. Zorzi,
coraliezorzi@gmail.com

Citation:

Zorzi, C., & de Vernal, A. (2024). Evolution of West-East contrast in the subarctic Pacific gyre during the Plio-Pleistocene based on palynological evidence at ODP Sites 882 and 887. *Paleoceanography and Paleoclimatology*, *39*, e2024PA004873. https://doi.org/10.1029/2024PA004873

Received 12 FEB 2024
Accepted 12 AUG 2024

Author Contributions:

Conceptualization: C. Zorzi
Formal analysis: C. Zorzi
Funding acquisition: A. de Vernal
Investigation: C. Zorzi
Methodology: C. Zorzi
Software: C. Zorzi
Supervision: A. de Vernal
Validation: A. de Vernal
Writing – original draft: C. Zorzi
Writing – review & editing: A. de Vernal

Abstract Fragmentary and contradictory evidence prevents a clear understanding of the possible role of the North Pacific Ocean surface on the ice-sheet evolution. New palynological data encompassing the Pliocene and Pleistocene at Ocean Drilling Program Site 882 in the northwest Pacific document sea-surface conditions from dinoflagellate cysts in addition to atmospheric trajectories from pollen grains and spores. The comparison of the Site 882 record with that of Site 887 from the northeast Pacific also permits documenting West to East contrasts across the subarctic North Pacific. The dinocyst assemblages at the two sites indicate strong temperature contrasts until 4.2 Ma, with much warmer conditions in the East. From 4.2 to 3.6 Ma, dinocyst assemblages of both sites are characterized by alternated dominance of the extinct taxa *Habibacysta tectata* and *Impagidinium detroitense* suggesting homogenous and cool conditions across the subarctic Pacific gyre. A major transition is recorded in the palynological assemblages at Site 882 around 2.7 Ma. It is marked by the highest occurrence of *Habibacysta tectata* and high percentages of *Filisphaera microornata* additionally to thermophilic taxa. Dinocyst record indicates high seasonality and warmer surface conditions due to reinforced stratification, which support the hypothesis of high evaporation at the origin of atmospheric moisture supply to high latitudes. During the last 1.2 Ma, the increase of *Operculodinium centrocarpum* relative to *Nematosphaeropsis labyrinthus* is tentatively interpreted as a reinforced influence of the subtropical waters. Hence, we suggest that the warm surface ocean fostered the inception and growth of northwestern North American ice-sheets during the Pliocene and Pleistocene.

1. Introduction

The evolution of sea surface conditions across the subarctic Pacific Ocean during the Pliocene and Pleistocene probably played an important role in the Northern Hemisphere ice-sheets development as evaporation over the ocean provided the water vapor supply necessary for precipitations at high latitudes. However, this is yet to be demonstrated, and this is the topic we address in the present paper. The onset of the present-day halocline in the subarctic Pacific was proposed to have occurred at about 2.7 Ma and to have been a key mechanism in the massive growth of ice sheets in the Northern Hemisphere during the late Pliocene (Haug et al., 1999, 2005; Sigman et al., 2004). However, the development of the halocline cannot be invoked for the inception of high-elevation glacier growth in North America as it occurred earlier, during the early Pliocene (Horikawa et al., 2015; Lagoe & Zellers, 1996; Reece et al., 2011; Sánchez-Montes et al., 2020). Other mechanisms were thus proposed, such as the uplift of the Alaskan Cordilleran (Duk-Rodkin et al., 2004) and/or higher sea surface temperature (SST) in the eastern Pacific compared to the West, which would have reinforced regional evaporation and precipitation (Sánchez-Montes et al., 2020). Yet, changes in zonal gradients of surface ocean temperature during the Pliocene remain unclear in geological archives. The Pliocene SSTs derived from U^{K}_{37} suggest warmer conditions in the West (~12°C according to Haug & Sarnthein, 2005) than in the East (~8°C after Sánchez-Montes et al., 2020), thus displaying a radically opposite scheme than the one proposed by modeling experiments suggesting warm conditions of ~15°C in the Gulf of Alaska (GoA) (Burls et al., 2017). In addition, contradictory evidence comes from the microfossil records. Radiolarian data led to suggest a persistent West-East surface ocean contrast in the subarctic Pacific since the mid-Miocene (Kamikuri et al., 2007; Morley & Nigrini, 1995) whereas the diatom data show consistent biostratigraphic schemes during the Pliocene and Pleistocene (Barron & Gladenkov, 1995), suggesting similar turnovers of the community likely in response to synchronous oceanic and/or climate changes affecting the surface waters in western and eastern subarctic Pacific.

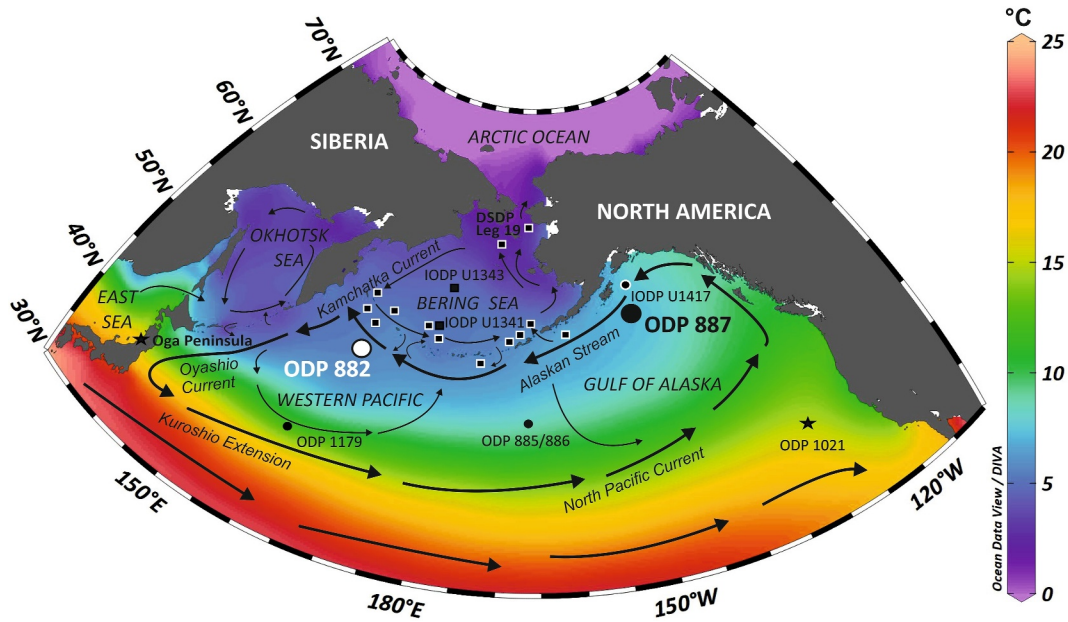

Figure 1. Northern North Pacific showing the annual sea surface temperature (°C) and the location of studied Site Ocean Drilling Program (ODP) 882 and of sites previously investigated for dinocyst and acritarch analyses in the Gulf of Alaska (Zorzi et al., 2020), the Bering Sea (Bujak, 1984; Bujak & Matsuoka, 1986; De Clercq, 2015; Matthiessen et al., 2018), the Shatsky Rise (Kanazawa et al., 2001) and offshore Japan (Matsuoka, 1983; Matsuoka et al., 1987), as well as the location of ODP Sites 1179, 885/886, 1021 and IODP Site U1417. Modern surface currents (Bonnet et al., 2012) are represented by black arrows. The map was prepared with Ocean Data View 4.7.7 (Schlitzer, 2016).

Well after the onset of Northern Hemisphere ice growth at 2.7 Ma (De Schepper & McClymont, 2023), the North Pacific was marked by an intensification of glaciation (cf. Barendregt & Duk-Rodkin, 2011) as reported from increased ice-rafted debris (IRD) in the subarctic gyre at the end of the Middle Pleistocene Transition (MPT), from ~1.25 to 0.75 Ma (Haug et al., 1999; Herbert, 2023; Rea & Snoeckx, 1995). The mechanisms at the origin of the amplification of glaciations at the MPT, when the climate cycle switched from dominant 41-kyr to 100-kyr cyclicity, are also a matter of debate (Mudelsee and Stattegger, 1997; Pisias & Moore, 1981). The closure of the Bering Strait due to an increase in regional sea-ice cover and low sea level during glacials was proposed as a trigger for enhancing the North Pacific Intermediate Water formation in the western North Pacific, which in turn contributed to lower atmospheric CO_2 and global cooling (Kender et al., 2018). A northward expansion of the subtropical gyre delivering more heat and moisture to high latitudes of the North Pacific was also proposed as a preconditioning mechanism for western North American ice sheet growth (Taylor et al., 2022).

So far, isolated and contradictory evidence in the subarctic Pacific has hampered a clear understanding of the possible effect of West-Est surface conditions on the development of regional ice sheets during the Pliocene and Pleistocene. Here, we developed a new record based on organic-walled microfossils, including dinoflagellate cysts (hereafter dinocysts) and acritarchs at the Ocean Drilling Program (ODP) Site 882 in the northwest Pacific Ocean. The study complements the record from ODP Site 887 in the northeast Pacific Ocean, which was established using an identical methodology (Figure 1; Zorzi et al., 2020). The dinocyst records from the two sites respectively located West and East of the subpolar gyre in the North Pacific, permitted us to reconstruct qualitatively past climate and oceanographic changes across the northern North Pacific and to assess the zonal gradients during the Pliocene and the Pleistocene. In addition, the examination of pollen grains and spores in samples from ODP Site 882 permitted us to estimate fluxes from land, which we interpreted as an indicator of wind transport.

2. Environmental Setting

The subarctic Pacific gyre is characterized by a cyclonic sea-surface circulation divided by two secondary gyres centered respectively in the western North Pacific Ocean and in the GoA (Figure 1; Favorite, 1976). The northern boundary of the subarctic gyre is delimited by the extent of the Alaska Stream, a westward current flowing from

Alaska to Kamchatka along the Aleutian and Commander Islands. Following the Siberian and Kamchatka Peninsula coasts, surface waters mix into the Kamchatka Current, originating from the Bering Sea and extending southward into the Oyashio Current off the Kuril Islands and Japan. The subarctic front, located from 40°N in the West to 50°N in the East constitutes the southern boundary of the gyre. It corresponds to a thermal barrier separating the cold and fresh water masses of the Subarctic Current from the warm and salty waters of the Kuroshio Expansion, which becomes wider (150 km) offshore the Emperor Seamounts, forming thereafter the North Pacific Current (Qiu, 2000). In addition, the subarctic front corresponds to the northern expansion of the Westerlies and the southern limit of the polar Easterlies (Gray et al., 2020).

In the subarctic Pacific, high rainfalls sustain low regional salinity in the upper water column, thus contributing to a sharp halocline above 120 m and making a physical barrier limiting nutrient and CO_2 vertical exchanges (Warren, 1983; Yuan & Talley, 1996). SSTs show large seasonal variation, from 10°C in summer to 4°C in winter, whereas surface salinity remains annually at about 32 ± 0.3 psu (Yuan & Talley, 1996; World Ocean Atlas; Boyer et al., 2013). The subarctic Pacific is a high nitrate, low chlorophyll region where the paucity of micronutrients such as iron limits primary productivity (Lam & Bishop, 2008). Higher marine productivity ~300 mg C m^{-2} day^{-1} in the West compared to the GoA (Honda et al., 2006) results in higher iron concentration (Nishioka et al., 2003) linked to inputs from proximal Asian dust sources (Mahowald et al., 2005) and volcanic rocks from the Kuril and Kamchatka margins (Lam & Bishop, 2008).

Modern dinocyst assemblages from the northwestern Pacific (NWP) are characterized by *Brigantedinium* spp. (up to 40%) with *Nematosphaeropsis labyrinthus*, cyst of *Pentapharsodinium dalei*, *Spiniferites elongatus* and *Islandinium minutum* with cyst concentrations ranging from 80 to 682 dinocysts.cm^{-3} (Bonnet et al., 2012). High percentages of *Brigantedinium* spp. and low cyst concentrations are compatible with low surface salinity and a sharp halocline (e.g., Bonnet et al., 2012; de Vernal et al., 2001; Rochon et al., 1999), which often corresponds to low primary productivity (Sigman et al., 2004).

3. Materials and Methods

3.1. Marine Sediments

Palynological analyses were performed on sediment samples from the ODP Hole 882A (50°21.79′N, 167° 35.99′E, 3,244 m) drilled on the Detroit Seamount in the northern part of the Hawaiian-Emperor Seamount Chain (Figure 1). Pliocene deposits are dominated by biogenic silica composed of diatom oozes while Pleistocene sediments are characterized by the alternation of diatom oozes and clayey diatom-rich mud with frequent occurrence of IRD (Rea et al., 1995). An important decrease in sedimentation rates is recorded at 105 m composite depth (mcd) due to a drop in the biogenic siliceous (Rea et al., 1995). For this study, we analyzed 44 samples collected between 353.2 and 8.3 mcd from Hole 882A, which encompasses 4.7 to 0.1 Ma (Table S1).

3.2. Age Model

The age model at ODP Site 882 is based on paleomagnetic reversals (Weeks et al., 1995) and fine tuning of bulk density variations with the orbital precession and summer insolation at 65°N (Tiedemann & Haug, 1995), which is consistent with independent biostratigraphic schemes based on diatoms (Barron & Gladenkov, 1995), radiolarians (Morley & Nigrini, 1995) and calcareous nannofossils (Barron et al., 1995). For this study, we calculated the age of each sample based on linear interpolations between the paleomagnetic reversals tie points used in the original age-depth model published by Barron et al. (1995). Here, ages of the Pliocene and the Pleistocene boundaries and paleomagnetic events were adjusted to the new chronology of the Plio-Pleistocene magnetic reversals redefined by Gibbard et al. (2010) and Ogg (2012). Hence, the Pliocene-Pleistocene boundary is defined by the Gauss-Matuyama geomagnetic reversal dated at 2.581 Ma (cf. Ogg, 2012) and recorded at 98.1 mcd in Hole 882A (9H-6, 85 cm) (Barron et al., 1995).

3.3. Palynological Analysis

Subsamples of 5 cm^3 of dry sediment were weighed and processed using standard palynological techniques used at Geotop, including sieving at 10 and 106 μm, in addition to repeated treatments with room temperature hydrochloric (10%) and hydrofluoric (48%) acids (de Vernal et al., 1996). No oxidation, alkali or ultrasound treatments were made. The residual fractions were mounted in glycerin jelly between microscope slides and

covers. A total of 44 samples were analyzed for their palynological contents using a transmitted light microscope at 250× to 1,000× magnification. The palynomorphs analyzed included dinocysts, acritarchs, pollen grains, and spores. One tablet of *Lycopodium* spores from Lund University was added at the beginning of the laboratory treatment for the calculation of concentrations and fluxes (Matthews, 1969; Mertens et al., 2009; Table S1). At least one slide of each sample was scanned with 2471 *Lycopodinium* spores and 111 marine palynomorphs counted on average. The total of dinocyst and acritarch identified per sample varies from 934 to 3 specimens. In parallel to dinocysts and acritarchs, a systematic identification of pollen grains and spores, mostly composed of *Picea* and *Pinus*, was performed to estimate total terrestrial palynomorph fluxes. Palynological raw counts are shown in Table S1. Samples with less than 30 identified specimens of dinocysts and acritarchs were excluded from the selected diagram (Figure 2) showing the relative proportion of dinocyst taxa recorded at least in 3 samples.

The taxonomy of Pliocene species is based on dinocyst investigations in the North Pacific by Matsuoka (1983), Bujak (1984), Bujak and Matsuoka (1986), and Zorzi et al. (2019, 2020). It is also based on studies undertaken in the North Atlantic by Head (1994), De Schepper (2006), De Schepper and Head (2009), De Schepper et al. (2004), and Hennissen et al. (2017). The list of extant and extinct taxa, with their taxonomical affinities at the family level (Gonyaulacaceae and Protoperidiniaceae) and their respective ecological preferences (warm, cool-to-cold water indicators, or characteristic of strong seasonal contrast) is provided with references in Table 1. We also identified two acritarchs, namely *Cymatiosphaera*? *invaginata* and *Lavradosphaera crista*.

3.4. Biostratigraphy

The biozonation follows the International Stratigraphic Guide (abridged version of Murphy & Salvador, 1999). The biozones are given informal names (NWP1 to NWP3) referring to the location of ODP Site 882 in the NWP. We distinguished the lowest and the highest occurrence (LO and HO), and the lowest and highest (LCO and HCO) common occurrence. The LO (or HO) corresponds to the oldest (or youngest) occurrence of a species, even if low counts are recorded. The LCO (or HCO) indicates the oldest (youngest) sample in which a given taxon is conspicuously abundant, although rare specimens can be recorded below (above). The sampling resolution has an impact on the accuracy of the estimated LO (HO) because the true age of the LO (HO) is between the lowest (highest) sample containing the species and the underlying (overlying) sample with (without) specimens.

The biozonation is supported by a constrained classical hierarchical clustering analysis based on the Simpson distance between samples, which helps to distinguish the main ecostratigraphic groups (Figure S1 in Supporting Information S1 and Figure 3). Cluster analysis was performed with the R environment (R Core Team, 2021) using the *Rioja* package (Juggins, 2020) and the CONISS methodology. The biozonation (Figure 3) includes all the samples analyzed in this study. The classification of relative abundance of dinocysts and acritarchs is as follows: *Rare to Frequent,* <10%, *Common*, 10%–29.9%, *Abundant*, 30%–49.9% and *Dominant,* >50%.

3.5. Indexes and Fluxes

The P/G = nP/(nP + nG) is the ratio between protoperidinioids (P) and gonyaulacoids (G) (Table 1). It is used as an index of marine productivity, but it may also relate to preservation since protoperidinioids are sensitive to oxidation (Zonneveld et al., 1997, 2007, 2008). The Shannon's diversity index is calculated using the software PAST (Hammer et al., 2005). In addition, the abundances of terrestrial and marine palynomorphs are expressed in terms of burial fluxes of palynomorphs for comparison of the fluctuations related to major changes in sediment accumulation. Smoothing curves constructed based on the *Astrochron* package for R (Meyers, 2019) highlight low-frequency variations.

4. Results

4.1. Main Features of Dinocyst Assemblages and Palynological Fluxes at ODP Site 882

In the studied sequence, the assemblages are characterized by 33 dinocyst species, including 23 extant and 10 extinct taxa, in addition to two acritarch taxa (Figure 2). Protoperidinioid cysts occur commonly in Pliocene and Pleistocene sediments together with gonyaulacoids (Figure 2; Table 1). The palynological record shows a higher temporal sampling resolution in the Pliocene section compared to the Pleistocene, with a mean of 0.13 Ma and 0.20 Ma between two consecutive samples, respectively (Table S1). Good preservation of palynomorphs in the

10.1029/2024PA004873

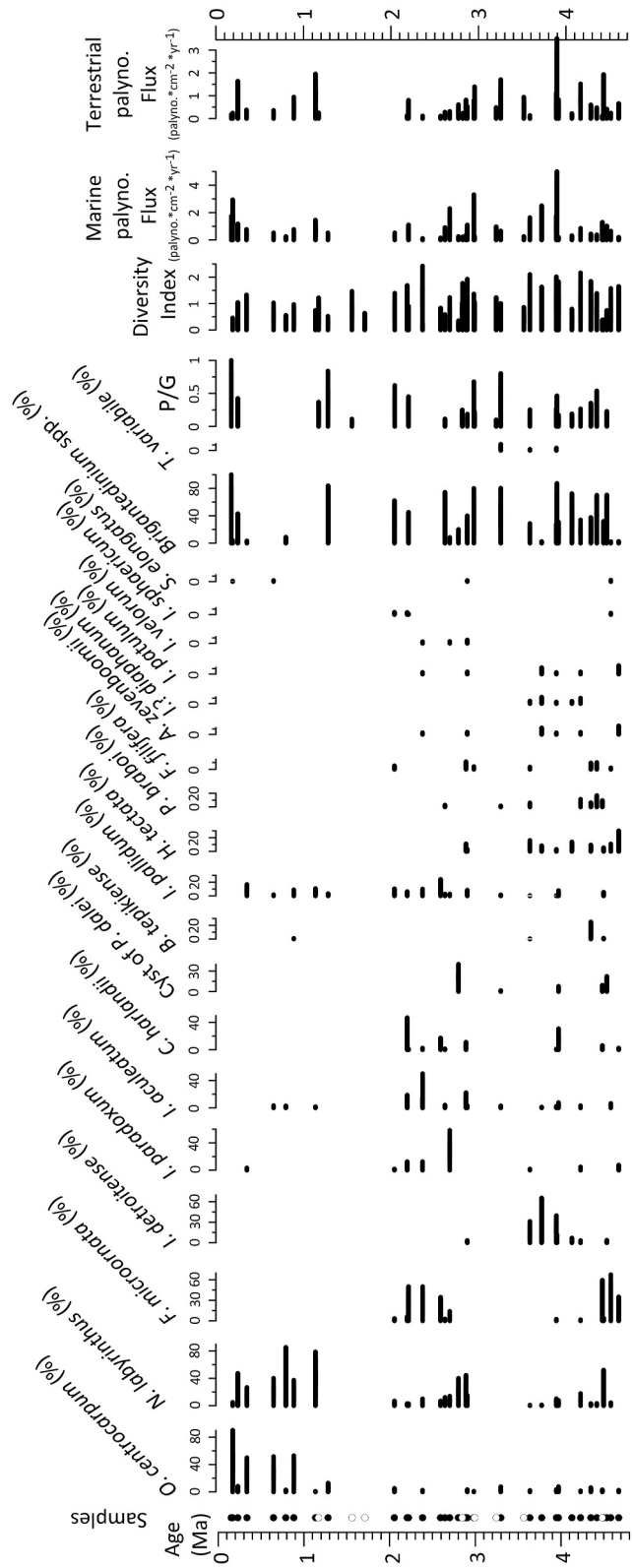

Figure 2. Relative abundance of dinocyst taxa in Plio-Pleistocene sediments at Ocean Drilling Program Site 882, protoperidinioid/gonyaulacoid (P/G), diversity index, and marine and terrestrial palynomorphs burial fluxes. Barren samples, whose percentages are excluded from this figure, are identified by open circles at the left of the diagram. Dinocyst names with abbreviations of genus names are given in Table 1.

Table 1
List of Dinocyst Taxa Recorded at Ocean Drilling Program Site 882 During the Pliocene and the Pleistocene, Showing Their Family Affiliation, Protoperidiniaceae (P), Gonyaulacaceae (G), Thoracosphaeraceae (T), and Their Ecological Affinities, Such as Warm, Cool-To-Cold, or Sensitive to Strong Seasonality

	Abbreviations.	Extinct	G	P	T	Warm	Cool-to-cold	Seasonality	References
Ataxiodinium choane	*A. choane*		X						Rochon et al. (1999), Zonneveld et al. (2013)
Ataxiodinium zevenboomii	*A. zevenboomii*	X	X			X			Head (1997), Limoges et al. (2020)
Bitectatodinium tepikiense	*B. tepikiense*		X				X	X	Radi and de Vernal (2004), Rochon et al. (1999), Hennissen et al. (2017)
Brigantedinium spp.	–			X					Rochon et al. (1999), Radi and de Vernal (2004)
Corrudinium harlandii	*C. harlandii*	X	X						Matsuoka (1983)
Corrudinium? *labradori*	*C.*? *labradori*	X	X						Head et al. (1989)
Cysts of *Pentapharsodinium dalei*	Cysts of *P. dalei*				X			X	Rochon et al. (1999), Van Nieuwenhove et al. (2020)
Cysts of *Protoperidinium americanum*	Cysts of *P. americanum*			X					Zonneveld et al. (2013), Radi and de Vernal (2004)
Filisphaera filifera	*F. filifera*	X	X				X		Matthiessen and Brenner (1996), De Schepper et al. (2011)
Filisphaera microornata	*F. microornata*	X	X				X	X	Hennissen et al. (2017), De Schepper et al. (2011)
Habibacysta tectata	*H. tectata*	X	X				X		Hennissen et al. (2017), De Schepper et al. (2011)
Impagidinium aculeatum	*I. aculeatum*		X			X			Radi and de Vernal (2004), Bonnet et al. (2012)
Impagidinium detroitense	*I. detroitense*	X	X						Zorzi et al. (2019)
Impagidinium? *diaphanum*	*I.* ? *diaphanum*	X	X						Zorzi et al. (2019)
Impagidinium japonicum	*I. japonicum*		X			X			Matsuoka (1983), Bonnet et al. (2012)
Impagidinium pallidum	*I. pallidum*		X				X		Rochon et al. (1999), Radi and de Vernal (2004), Bonnet et al. (2012)
Impagidinium paradoxum	*I. paradoxum*		X			X			Zonneveld et al. (2013), Bonnet et al. (2012)
Impagidinium patulum	*I. patulum*		X			X			Rochon et al. (1999), Radi and de Vernal (2004), Bonnet et al. (2012)
Impagidinium sphaericum	*I. sphaericum*		X			X			Zonneveld et al. (2013), Bonnet et al. (2012), Penaud et al. (2008)
Impagidinium velorum	*I. velorum*		X			X			Rochon et al. (1999), Bonnet et al. (2012)

Table 1
Continued

	Abbreviations.	Extinct	G	P	T	Warm	Cool-to-cold	Seasonality	References
Nematosphaeropsis labyrinthus	*N. labyrinthus*		X						Rochon et al. (1999), Zonneveld et al. (2013), Bonnet et al. (2012)
Operculodinium centrocarpum	*O. centrocarpum*		X						Rochon et al. (1999), Bonnet et al. (2012)
Pyxidinopsis braboi	*P. braboi*	X	X				X		Hennissen et al. (2017), De Schepper et al. (2011)
Pyxidinopsis reticulata	*P. reticulata*		X						Zonneveld et al. (2013), Bonnet et al. (2012)
Quinquecuspis concreta	*Q. concreta*			X					Zonneveld et al. (2013), Radi and de Vernal (2004)
Selenopemphix dionaeacysta	*S. dionaeacysta*	X		X					Head et al. (1989)
Selenopemphix nephroides	*S. nephroides*			X		X			Zonneveld et al. (2013)
Spiniferites elongatus	*S. elongatus*		X				X		Rochon et al. (1999), Zonneveld et al. (2013)
Spiniferites membranaceus	*S. membranaceus*		X			X			Rochon et al. (1999), Zonneveld et al. (2013)
Spiniferites mirabilis	*S. mirabilis*		X			X			Zonneveld et al. (2013)
Spiniferites ramosus	*S. ramosus*		X			X			Rochon et al. (1999), Zonneveld et al. (2013)
Trinovantedinium variabile	*T. variabile*			X					Bonnet et al. (2012)
Xandarodinium xanthum	*X. xanthum*			X					Head (1997)

sediment, or at least no selective degradation, is suggested by common occurrences of protoperidinioid cysts and high values of the P/G ratio in the study sequence (Figure 2), except for the 1.9–1.2 Ma interval during which a very low number of marine palynomorph was recorded, with 3–62 specimens identified per sample (mean of 23; Table S1). Low marine palynomorph concentrations in this interval, including 3 barren samples, may result from a drop in marine productivity, preservation issues, or a combination of both, which prevents reliable interpretation of paleoenvironmental conditions. Burial fluxes of marine and terrestrial palynomorphs were generally higher in the Pliocene compared to the Pleistocene (Figure 2), although the differences are not significant (*t*-test, $p = 0.13$ and 0.28 respectively). Maximum pollen grain and spore inputs occurred through the 4.7 to 4.0 Ma interval and progressively decreased until 2.7 Ma to reach its lowest values during the Pleistocene.

In the Pliocene sediment, the dinocyst assemblage is characterized by high percentages of *Filisphaera microornata, Impagidinium detroitense* and *Brigantedinium* spp., with a diversity index ranging from 1 to 2 (Figure 2). Until 4.4 Ma, the marine palynomorph record is characterized by the occurrence of *F. microornata* with moderate percentages of *Habibacysta tectata*. Between 4.4 and 4.2 Ma, high percentages of *Brigantedinium* spp. are recorded in association with *Pyxidinopsis braboi*, *F. filifera* and *Nematosphaeropsis labyrinthus*. From 4.2 to 3.6 Ma, an increase in *I. detroitense* with low to moderate percentages of *H. tectata*, *I. aculeatum*, *Ataxiodinium zevenboomii*, *I.*? *diaphanum* and *I. patulum* parallels the decrease in *Brigantedinium* spp..

During the late Pliocene and early Pleistocene, from 2.9 to 1.9 Ma, the composition of the dinocyst assemblage was characterized by *I. paradoxum, I. aculeatum, Corrudinium harlandii, I. velorum, I. sphaericum* and *I. pallidum*. The diversity index was high (>1). There was an important change in dinocyst assemblages marked by an increase in *F. microornata* relative to *N. labyrinthus* at about 2.7 Ma.

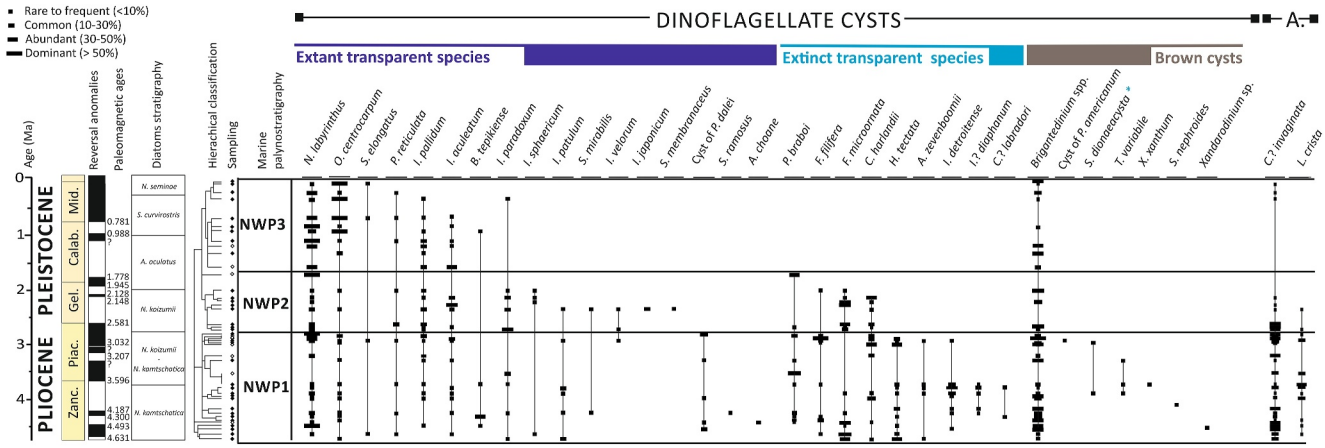

Figure 3. Pliocene and Pleistocene biozone boundaries at Ocean Drilling Program (ODP) Site 882. The relative abundance of modern and extinct marine palynomorphs, including dinocyst and acritarch, are classified according to four categories: rare to frequent, <10%, common, 10%–29.9%, abundant, 30%–49.9% and dominant, >50%. The open diamonds next to the hierarchical classification indicate samples in which less than 30 specimens were identified. The magnetic anomalies and diatom biozones at ODP Site 882 are from Barron et al. (1995). Abbreviations are NWP for northwestern Pacific, A. for Acritarch, Zanc. for Zanclean, Piac. for Piacenzian, Gel. for Gelasian, Calab. for Calabrian, Mid. for Middle Pleistocene. Marine palynomorph abbreviations are defined in Table 1.

In the upper part of the sequence encompassing the last 1.2 Ma, dinocyst assemblages were exclusively composed of extant taxa, which are also recorded in the modern sediments of the North Pacific, such as *Operculodinium centrocarpum, N. labyrinthus* and *I. pallidum* (Figure 2; Bonnet et al., 2012). In addition, a progressive replacement of dominant species is recorded with the increase of *O. centrocarpum* relative to *N. labyrinthus*.

4.2. Dinocyst and Acritarch Biostratigraphy of ODP Site 882

The dinocyst assemblages and hierarchical cluster analysis led to the definition of three major biozones encompassing the Pliocene and Pleistocene (Figure 3; Figure S1 in Supporting Information S1). The main biostratigraphic boundaries at ODP Site 882, including those from dinocysts and acritarchs (this study) and diatoms (Barron & Gladenkov, 1995), provide an overview of planktonic population turnovers (see Table S2 and Text S1 in Supporting Information S1 for a formal description and detailed comparison of dinocysts, diatom and radiolarian bio-events from ODP Holes 882 A and B).

The NWP1 biozone corresponds to the body of strata whose uppermost limit is defined by the HO of *Habibacysta tectata*. Additional events characterizing the top of the zone are the HO of *Ataxiodinium zevenboomii* and *Selenopemphix dionaeacysta*. The biozone is characterized by a high proportion of extinct species, including *Impagidinium detroitense*, *H. tectata, Filisphaera microornata, F. filifera* and *Pyxidinopsis braboi*. The acritarch *Cymatiosphaera*? *invaginata* is common to dominant while *Lavradosphaera crista* is regularly recorded in few abundances (Figure 3). The NWP1 biozone encompasses the early and the late Pliocene, from 4.67 to 2.80 ± 0.10 Ma and combines 24 samples with a temporal resolution ranging from 0.02 to 0.26 Ma (mean of 0.13 Ma).

The biozone NWP2 extends from the HO of *H. tectata* to the HO of *P. braboi*. Additional events characterizing the top of the zone are the HO of *F. microornata* and *F. filifera*. This biozone is characterized by the decrease of extinct species and the relative increase of extent dinocysts. The NWP2 biozone, including 9 samples with a temporal resolution from 0.06 to 0.34 Ma (mean of 0.19 Ma), encompasses the late Piacenzian and early Calabrian from 2.70 ± −0.09 to 1.71 ± 0.35.

The NPW3 biozone is defined between the HO of *P. braboi* and an undefined position at or above the top of the section analyzed. This zone is exclusively composed of modern dinocysts, including *N. labyrinthus, Impagidinium pallidum* and *Operculodinium centrocarpum* while the acritarch *C.*? *invaginata* is absent to frequent. The NWP3 biozone encompasses the early Calabrian to present, between 1.56 ± 0.38 to 0 Ma and gathers 11 samples with a temporal resolution fluctuating between 0.06 and 0.31 Ma (mean of 0.21 Ma).

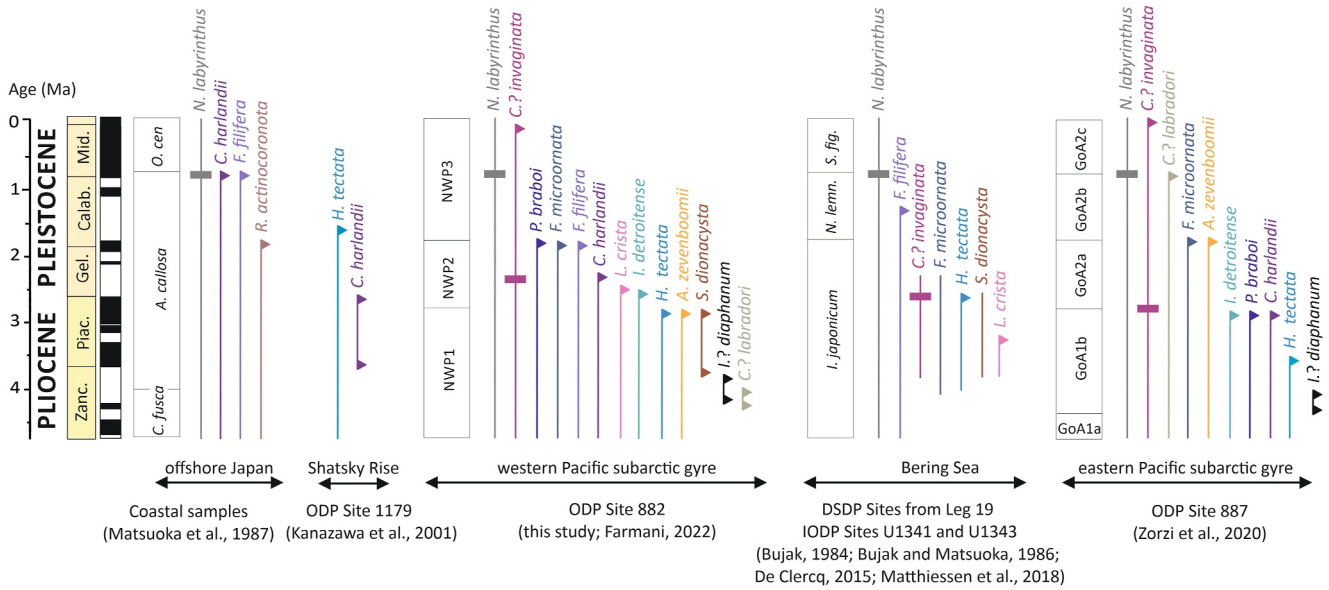

Figure 4. Compilation of published dinoflagellate cyst and acritarch biozonations off Japan (Matsuoka et al., 1987), in the Bering Sea (Bujak, 1984; Bujak & Matsuoka, 1986) and the Gulf of Alaska (Zorzi et al., 2020) compared with that of Ocean Drilling Program (ODP) Site 882 in northwestern Pacific (this study). This synthesis shows events identified by targeted studies, such as the highest occurrence (HO) of *H. tectata* at ODP Site 1179 in the Shatsky Rise (Figure 1; Kanazawa et al., 2001) and of *F. filifera* from IODP Hole U1343 E in the Bering Sea (Figure 1; Matthiessen et al., 2018), as well as biostratigraphic events such as the HO of *I. detroitense* at OPD Site 882 (Farmani, 2022) and the occurrence of *S. dionaeacysta*, *L. crista* and *C.*? *invaginata* at Hole U1341 B in the Bering Sea (Figure 1; De Clercq, 2015). The HO of taxa are represented by triangles, while the highest common occurrence is represented by rectangles. Abbreviations are as follows: Zanc. for Zanclean, Piac. for Piacenzian, Gel. for Gelasian, Calab. for Calabrian, Mid. for Middle Pleistocene. Dinocyst and acritarch abbreviations are defined in Table 1.

5. Discussion

5.1. Comparison of the New Biozonation of ODP Site 882 With Existing Dinocyst Records

5.1.1. Existing Palynological Records and Limitations of the Approach

Few studies have investigated dinocyst and acritarch records in the Pacific Ocean compared to the Atlantic Ocean and adjacent seas. Nevertheless, the analysis of surface sediments has permitted assessing the value of dinocysts for regional paleoceanographic reconstructions throughout the late Quaternary (de Vernal & Pedersen, 1997; Marret et al., 2001) demonstrating that the North Pacific assemblage composition is strongly controlled by seasonal SST (Bonnet et al., 2012; Pospelova et al., 2008) and regional primary marine productivity (Pospelova et al., 2008; Radi & de Vernal, 2004, 2008).

In this study, we attempted to compare our marine palynomorph biozonation of ODP Site 882 with existing dinocyst records from the subarctic Pacific to identify possible common climate and/or oceanic changes in the marine ecosystem of the North Pacific during the last 5 Ma. Our comparison combines Pliocene and Pleistocene records from southern, central (Bujak, 1984; Bujak & Matsuoka, 1986), eastern and northern Bering Sea (Matsuoka & Bujak, 1988), offshore Japan (Kurita & Obuse, 2003; Matsuoka, 1983; Matsuoka et al., 1987), as well as from the GoA (Zorzi et al., 2020) (Figures 1 and 4). However, most of the pioneer studies suffer from a sparse sampling resolution, poor age control and uncertain taxonomic assignments, which makes the comparison between records difficult. Hence, we also compared our results with those from recent biostratigraphic studies performed with high temporal resolution but encompassing targeted intervals based on cores collected in the Bering Sea (De Clercq, 2015; Haj Soltan, 2021; Matthiessen et al., 2018) and the western Pacific (Farmani, 2022; Kanazawa et al., 2001) (Figures 1 and 4). These studies included dinocysts described after the late 1980s (De Schepper & Head, 2009; De Schepper et al., 2004; Head et al., 1989; Head, 1994, 1997, 1998, 2000; Head & Norris, 2003; Head & Wrenn, 1992; Marret et al., 2001; Verhoeven & Louwye, 2013; Zorzi et al., 2019) in addition to taxonomic revisions of problematic cyst such as *Filisphera pilosa* and *Nematosphaeropsis lemniscata* (Head & Wrenn, 1992; Head et al., 1994; Rochon et al., 1999).

5.1.2. Synchronous Boundaries in the North Pacific and Paleoceanographic Implications

In the North Pacific, the earliest synchronous biostratigraphic boundary of the Pliocene and Pleistocene occurred at ~2.7 Ma, which corresponds to the top of the NWP1 biozone at ODP Site 882 and with the top of the GoA1 biozone at ODP Site 887 (Figures 1 and 4; Zorzi et al., 2020). The corresponding bioevents include the HO of *Habibacysta tectata*, *Ataxiodinium zevenboomii* and *Selenopemphix dionaeacysta* at ODP Site 882, and the HO of *Impagidinium detroitense*, *Pyxidinopsis braboi* and *Corrudinium harlandii* and the LCO of *Cymatiosphaera*? *invaginata* at ODP Site 887 (Figure 4). A biostratigraphic turnover such as the one we noticed based on dinocysts and acritarchs was also recorded using diatom data from the subarctic Pacific gyre (Figure 3; Text S1; Table S2 in Supporting Information S1; Barron & Gladenkov, 1995). Turnovers occur concurrently with the onset of the modern halocline in the subarctic Pacific, initially evidenced at 2.7 Ma by a shift of the biogenic opal accumulation and sedimentary nitrogen isotopic composition of ODP Site 882 (Haug et al., 1999).

A boundary at 1.7 Ma, which corresponds to the top of biozone NWP2, is expressed in all dinocyst records from the subarctic Pacific (Figure 4; Bujak, 1984; Bujak & Matsuoka, 1986; Matsuoka et al., 1987; Zorzi et al., 2020). It correlates with the top of zone GoA2a at ODP Site 887 in the eastern subarctic Pacific (Figures 1 and 4; Zorzi et al., 2020) and of the *Nematosphaeropsis lemniscata* zone in the Bering Sea (Figures 1 and 4; Bujak, 1984; Bujak & Matsuoka, 1986). The biostratigraphic boundary at 1.7 Ma is defined by the mutual HO of *F. microornata* in the subarctic gyre, respectively associated to the HO of *P. braboi* and *F. filifera* at ODP Site 882 and to the HO of *A. zevenboomii* at ODP Site 887 (Figure 4; Zorzi et al., 2020), while it is distinguished in the Bering Sea based on the HO of *I. japonicum*, *Lejeunecysta fallax*, *Tuberculodinium vancampoae*, *I. velorum*, *Tectatodinium pellitum* and *Spiniferites hexatypicus* (Figure 4; Bujak, 1984; Bujak & Matsuoka, 1986). Off Japan, the top of the NWP2 biozone correlates to the middle part of the *Achomosphaera callosa* zone (Figure 4; Matsuoka, 1983; Matsuoka et al., 1987), which is a stratigraphic boundary that possibly coincides with the HO of several dinocyst taxa reported by Matsuoka et al. (1987), including *I. velorum* and *Reticulatosphaera actinocoronata*. While the biostratigraphic boundary at 1.7 Ma is marked by different dinocyst and acritarch taxa throughout the North Pacific, the regional disappearance of species seems to have mostly impacted those having ecological affinities for warm and/or high salinity conditions. These species include *A. zevenboomii* (Head, 1997), *I. velorum* (Bonnet et al., 2012), *I. japonicum* (Bonnet et al., 2012), *R. actinocoronata* (Schreck et al., 2017), *S. hexatypicus* (Matsuoka, 1983) and *L. fallax* (Head & Norris, 2003). The disappearance of species sensitive to high seasonal temperature and salinity contrasts, such as *F. microonata* (Hennissen et al., 2017), also suggests a shift toward colder and/or less saline conditions.

5.2. Evolution of the West-East Gradient in the Subarctic Pacific During the Plio-Pleistocene

5.2.1. Strong Sea Surface Regionalism Before 4.2 Ma

From 4.7 to 4.2 Ma, dinocyst assemblages at ODP Site 882 are characterized by high percentages of *Filisphaera microornata*, an extinct species also recorded in Pliocene sediments of the Labrador Sea (Head et al., 1989, 1994), the Baffin Bay (Aubry et al., 2020) and the North Atlantic Ocean (Hennissen et al., 2017). The assemblage of this early Pliocene interval is characterized by *Brigantedinium* spp., an euryhaline opportunistic genus that is abundant in the northern North Pacific and the Bering Sea today (Bonnet et al., 2012), in addition to some occurrences of the cool-tolerant *Habibacysta tectata* and the cold-waters *Pyxidinopsis braboi* and *F. filifera* retrieved during the 4.7–4.2 Ma interval (Figure 2; Table 1). Despite uncertainties on the ecological requirements of extinct species, such an assemblage indicates cool sea-surface conditions, compatible with the low SST estimates of ~11°C from U^{K}_{37} data at ODP Site 882 (Figure 5b; Haug & Sarnthein, 2005). A decreased abundance of *F. microornata* relative to *Brigantedinium* spp. is recorded at 4.4 Ma (Table 1; Figure 2) suggesting a change in sea-surface conditions, which is not depicted in the U^{K}_{37} record (Figure 5; Haug et al., 2005), but might relate to trophic changes in the upper water column. The distribution of the heterotrophic *Brigantedinium* genus is largely controlled by its prey supplies, including diatoms, blooming with elevated nutrients (Dale, 1996). An increase in the opportunistic *Brigantedinium* spp., in addition to *P. braboi*, which is sensitive to nutrients (Hennissen et al., 2017), may reflect a very productive ecosystem, consistently with high biogenic opal recorded at ODP Site 882 (Figure 5d; Haug et al., 2005).

In the eastern subarctic Pacific, at ODP Site 887 (Figure 1), the 4.7 to 4.2 Ma Ma interval is characterized by the highest percentages of thermophilic dinocyst taxa, up to 25% (Figure 5h). These taxa include *Ataxiodinium zevenboomii*, *Impagidinium velorum*, and *I. patulum* (Table 1). These and the few occurrences of *F.*

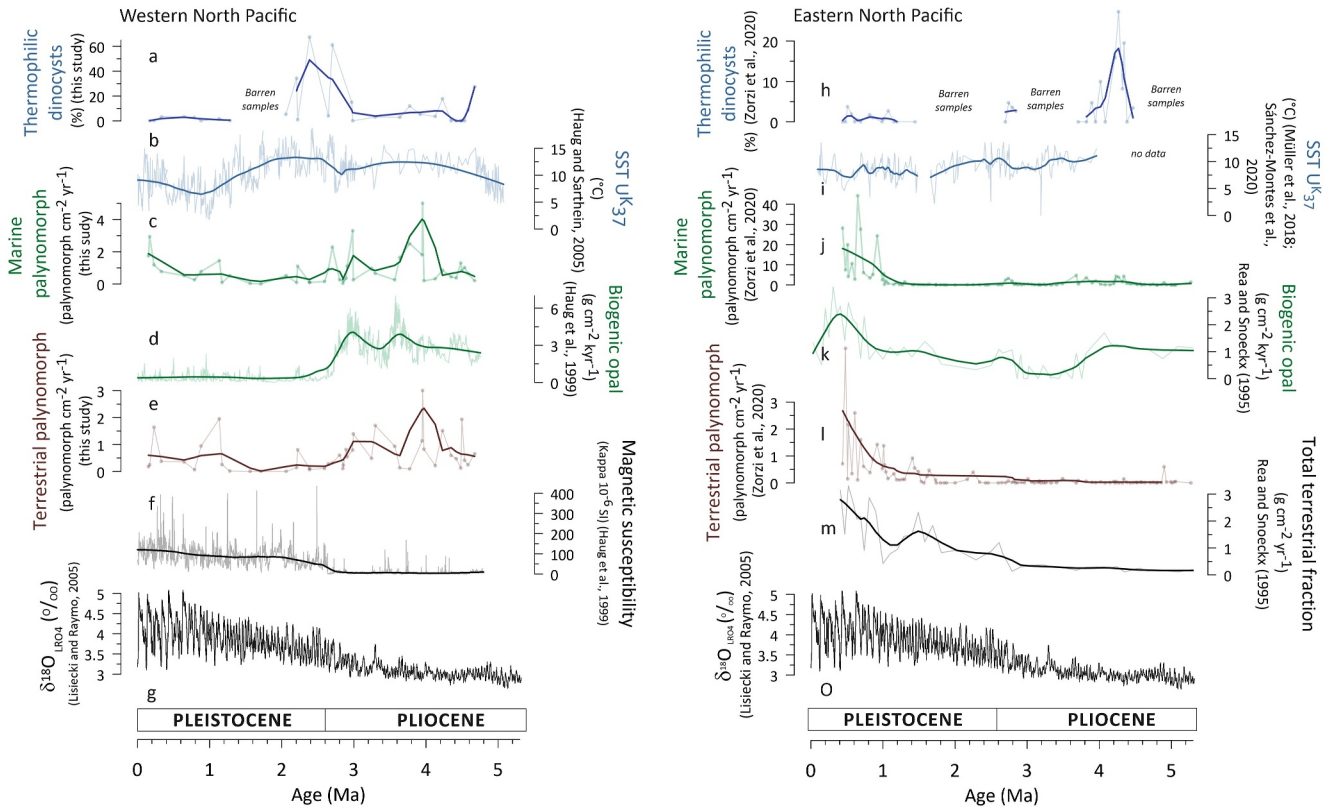

Figure 5. Synthesis of marine and terrestrial proxies in western (a–f) and eastern (h–m) subarctic Pacific. The percentages of thermophilic dinocyst species at Ocean Drilling Program (ODP) Sites 882 (a) and 887 (h) (Figure 1) contain *Ataxiodinium zevenboomii, Impagidinium aculeatum, Impagidinium japonicum, Impagidinium paradoxum, Impagidium patulum, Impagidinium sphaericum, Impagidinium velorum, Selenopemphix nephroides, Spiniferites membranaceus, Spiniferites mirabilis* and *Spiniferites ramosus* (see Table 1). The sea-surface temperature (b and i) estimates based on U^{K}_{37} are from Haug and Sarnthein (2005) at ODP Site 882, and from Müller et al. (2018) and Sánchez-Montes et al. (2020) at IODP Site U1417 (Figure 1). Marine productivity proxies include the fluxes of marine palynomorphs combining dinocysts and acritarchs (c and j; this study, Zorzi et al., 2020), and biogenic opal (d and k; Haug et al., 1999; Rea & Snoeckx, 1995) at ODP Sites 882 and 887 (Figure 1). The terrestrial palynomorphs include pollen and spores (e and l; this study; Zorzi et al., 2020) from ODP Site 882 and 887. Magnetic susceptibly and terrestrial fraction of marine sediments recording the amount of ice-rafted debris (f and m) are from Rea and Snoeckx (1995) and Haug et al. (1999) at ODP Sites 882 and 887 respectively. Fluctuation of the $\delta^{18}O_{benthic\ LRO4}$ is presented at the bottom of Figure (g and o) (Lisiecki & Raymo, 2005). Data sets are displayed in transparency lines while smoothing curves, highlighting the long-term trend, are shown as solid lines.

microornata, *B. tepikiense* and *P. braboi* suggest temperate conditions (Zorzi et al., 2020). Although there is no U^{K}_{37} data from the GoA (Figure 5i), which prevents a direct comparison, U^{K}_{37}-based SST reconstruction at ODP Site U1021 located in the northeast Pacific (39°N) (Figure 1), reveals warm sea-surface conditions (LaRiviere et al., 2012). Hence, dinocyst assemblages and derived SST document strong temperature contrasts with cold-to-cool conditions in the West and temperate conditions in the East as previously suggested by Burls et al. (2017) based on numerical modeling. Therefore, our results support the hypothesis of a strong zonal gradient of temperature that has (a) favored deep-water formation and active Pacific meridional circulation in the western subarctic Pacific (Burls et al., 2017) and (b) increased evaporation in the eastern Pacific, fostering the early growth of Alaskan mountain glaciers during the early Pliocene, in turn resulting in seasonal meltwater released to the Bering Sea (Horikawa et al., 2015).

5.2.2. Reduction of the Zonal Temperature Contrast at 4.2 Ma

From 4.2 to 3.6 Ma, dinocyst assemblages at ODP Sites 882 and 887 are both characterized by the extinct taxa *I. detroitense* and *H. tectata* accompanied by a few thermophilic dinocyst species namely *A. zevenboomii, I. patulum* and *I. aculeatum* (Figures 2 and 5a; Table 1; Zorzi et al., 2020). Dinocyst assemblages are similar at both sites, which led us to suggest homogenous sea-surface conditions across the subarctic Pacific gyre. High percentages of *I. detroitense*, likely endemic to the North Pacific, along with the extinct *H. tectata*, indicate non-

analogous oceanographic conditions between 4.2 and 3.6 Ma. Although the ecological requirement of *I. detroitense* remains uncertain, the common occurrence of *H. tectata*, interpreted as a cool-tolerant taxon in the North Atlantic (Table 1) likely reflects cool conditions. Reduction of the zonal contrast parallels the long-term persistence of cool conditions with derived U^{K}_{37} SST of about 11°C in the western North Pacific (Figure 5b; Haug & Sarnthein, 2005) and 10°C in the eastern North Pacific (Figure 5i; Sánchez-Montes et al., 2020). Thus, dinocyst and alkenone data evidence together a reduction of the zonal contrast in sea-surface temperature after 4.2 Ma in the subarctic Pacific.

5.2.3. Toward the Onset of Major Glaciations During the Late Pliocene

An increase in *F. microornata* relative to the cosmopolitan *N. labyrinthus* is recorded at 2.7 Ma. From 2.7 to 2.2 Ma, this change is accompanied by the highest percentages of thermophilic species, including *I. velorum, I. aculeatum, I. paradoxum, Spiniferites membranaceus* and *S. mirabilis* reaching maxima up to 67% of the dinocysts assemblage, at 2.4 Ma (Figures 2 and 5a; Table 1). In the North Atlantic Ocean and adjacent seas, the distribution of *F. microornata* was related to reduced salinity and high seasonal contrasts of temperatures (Hennissen et al., 2017; Table 1). Its increase at 2.7 Ma in the western North Pacific, together with high percentages of thermophilic species, may reflect reinforced seasonality with warmer but less saline surface waters.

Despite a lower temporal resolution, the dinocyst record is consistent with high seasonal contrasts of SST, with warmer conditions during late summer/autumn, as indicated based on U^{K}_{37} (Figure 5b; Haug & Sarnthein, 2005; Haug et al., 2005) and colder temperatures during winter/early spring, as indicated from $\delta^{18}O_{G.\ bulloides}$ (Haug et al., 2005; Maslin et al., 1998). Reinforced seasonality has been associated with the development of the permanent halocline at 2.73 Ma, which enhanced upper water stratification due to reduced sea-surface salinity (Haug et al., 2005). We thus suggest that dinocyst assemblages, isotopic data and U^{K}_{37}-based SST result from reduced salinity surface waters and warm late summer/autumn surface waters in a context of high seasonality in the western subarctic Pacific. Warm conditions, at least seasonally, could have provided the atmospheric moisture supply and precipitation necessary for the intensification of the glaciations at the high latitudes of the North Pacific (Haug et al., 2005).

The development of the halocline in the northern Pacific has initially been deduced from an abrupt decrease in the biogenic opal accumulation (Figure 5d; Haug et al., 1999) and increased isotopic composition of nitrogen at ODP Site 882 (Haug et al., 1999). These changes have been interpreted as the result of a drop in biological production in response to a reduced flow of nutrient-rich deep water to the euphotic zone (Haug et al., 1999; Sigman et al., 2004). Diatom (Barron & Gladenkov, 1995; Shimada et al., 2009) and radiolarian records (Kamikuri et al., 2007) support the decrease in marine productivity related to reduced nutrient availability. However, marine palynomorph fluxes have shown similar values from the mid-Pliocene, except for two occasional peaks at 2.70 and 2.98 Ma (Figure 2). In addition, the heterotrophic *Brigantedinium* spp., reflecting a productive environment, is occasionally recorded after 2.73 Ma, alternating with high percentages of the thermophilic species. The composition of assemblages and fluxes of dinocysts show little evidence of the nutrient drop suggested by siliceous microfossil, sedimentary and geochemical records at ODP Site 882. Thus, the dinocyst assemblages rather indicate that a productive ecosystem could have developed episodically after the halocline onset. Alternated high percentages of *Brigantedinium* spp. and *F. microornata* with thermophilic species possibly recorded the alternate of glacial and interglacial climate conditions, but the low sampling resolution of dinocyst record does not permit strong assessment.

Finally, the palynological record of ODP Site 882 shows a progressive decrease in pollen grains and spores between 3.0 and 2.7 Ma (Figure 5e). In the sedimentary context of the study site located on a seamount, the absence of IRD, concomitant with maximum inputs of pollen grains (Haug et al., 1999; Figures 5e and 5f), mostly the airborne *Picea* and *Pinus* (Table S1), suggests important fluxes related wind transport. Thus, the progressive decrease in total terrestrial palynomorphs recorded during the late Pliocene, can be interpreted as a change in the wind transport and/or in the forest cover in the adjacent land. The decrease in terrestrial palynomorphs fluxes is consistent with a progressive southward migration of the westerlies during the late Pliocene based on dust records at ODP Sites 1208 and 885/886 (Figure 1; Abell et al., 2021), resulting in a contraction and strengthening of the Hadley Cell. This atmospheric pattern would have favored the moisture transport from low to high latitudes, which in turn acted as a preconditioning mechanism, decreasing the surface water salinity in the subarctic gyre and thus fostering the halocline onset (Burls et al., 2017).

5.2.4. Cooling of the North Pacific at 1.7 Ma

After 1.7 Ma, only modern dinocyst taxa are recorded at ODP Site 882 (Figure 2). They include *I. pallidum* and *S. elongatus*, in addition to *Brigantedinium* spp., *N. labyrinthus* and *O. centrocarpum* (Figure 2), which together suggest cool subpolar conditions as in the modern North Pacific Ocean (Bonnet et al., 2012). Low percentages of thermophilic taxa and low species diversity in dinocyst assemblages indicate cooler conditions compared to the earlier part of the Pleistocene as also suggested by the U^{K}_{37}-derived SST (Figures 2, 5a, and 5b; Haug & Sarnthein, 2005). Hence, a major oceanic cooling seems to be recorded at 1.7 Ma throughout the North Pacific (cf. Section 5.1.2), including the GoA (Figures 5h and 5i; Shimada et al., 2009; Müller et al., 2018; Zorzi et al., 2020), the Bering Sea (Bujak & Matsuoka, 1986; Stroynowski et al., 2015) and offshore Japan (Matsuoka et al., 1987). This cooling coincides with the massive IRD increase at ODP Site 887 related to discharge of the North American ice-sheet (Figure 5m; Rea & Snoeckx, 1995).

In the GoA, both biogenic opal and marine palynomorph fluxes rose after 1.8 Ma (Figures 5j and 5k; Rea & Snoeckx, 1995; Zorzi et al., 2020). Increased marine productivity at ODP Site 887 was accompanied by the highest terrestrial palynomorph and IRD fluxes (Figures 5k and 5l; Zorzi et al., 2020), illustrating linkages between glacial discharge and ocean fertilization (Duprat et al., 2016; Müller et al., 2018). Hence, the palynological data may suggest high productivity as the result of vertical mixing and nutrient resuspension toward the surface induced by meltwater discharge at the base of tidal glaciers (e.g., Meire et al., 2016). In the context of a stratified open ocean, such a mechanism may have fostered phytoplankton growth in the GoA by delivering local macronutrients and micronutrients (Sánchez-Montes et al., 2022). In the western subarctic Pacific, in the contrary, low marine productivity was recorded as indicated both by marine palynomorphs and biogenic opal fluxes at ODP Site 882 (Figures 5c and 5d; this study; Haug et al., 1999) suggesting distinct mechanisms controlling the subarctic primary productivity at local to regional scales, in the eastern and western Pacific.

5.2.5. Progressive Oceanic Change During the Middle-Late Pleistocene

During the last 1.2 Ma, a significant increase of *O. centrocarpum* relative to *N. labyrinthus* is recorded at ODP Site 882, distinguishing the pre-from post-MPT assemblages (Figure 2). Important changes in assemblages were concurrently observed offshore Japan (Matsuoka et al., 1987) and in the GoA (Zorzi et al., 2020). The percentage of thermophilic species at both ODP Sites 882 and 887 remained low (Figures 5a and 5h). The ecological significance of this change is difficult to assess because the dominant taxa, *O. centrocarpum* and *N. labyrinthus,* are cosmopolitan and widely distributed (Table 1; Bonnet et al., 2012; de Vernal et al., 2020). Nevertheless, the increase of *O. centrocarpum* in the western Pacific has been used as an indicator of the Kuroshio water mass (Balota et al., 2021) questioning the possible increased influence of the subtropical water masses into the subarctic Pacific gyre during the late Pleistocene. The northward migration of the subtropical water masses was probably a mechanism critical for delivering the heat and moisture to the high latitudes of the northwest Pacific feeding the post-MPT ice-sheets (Matsuzaki et al., 2015; Taylor et al., 2022).

6. Conclusions

The new record of dinocysts and acritarchs at ODP Site 882 led us to define biostratigraphic boundaries at 2.7 and 1.7 Ma. These are marked by the HO of *Habibacysta tectata* and *Pyxidinopsis braboi* respectively. Beyond their importance in terms of biodiversity change, these boundaries correspond to major paleoceanographical transitions. The comparison with previous dinocyst studies from the GoA (Zorzi et al., 2020), the Bering Sea (Bujak & Matsuoka, 1986) and off Japan (Matsuoka et al., 1987) allowed us to document large-scale features in the dinocyst and acritarch distribution, which we interpreted as the response to major oceanographic and/or climate changes with the onset of permanent subarctic halocline at 2.7 Ma and a large-scale North Pacific cooling at 1.7 Ma.

Our palynological study documents the evolution of West-East gradients in surface waters of the subarctic Pacific during the last 5 Ma. Evidence comes from dinocyst assemblages, which suggest cool-to-cold surface waters in the western Pacific and temperate conditions in the eastern Pacific, thus strong zonal contrast of temperatures in the subarctic Pacific until about 4.2 Ma. Warmer conditions in the east compared to the west may have fostered the onset of glaciations of the Alaska Peninsula during the early Pliocene. After 4.2 Ma, the significant increase of *Impagidinium detroitense* and *Habibacysta tectata* both in the western and eastern subarctic Pacific is interpreted as the result of a reduction of zonal contrast. At 2.7 Ma, an increase in *Filisphaera microornata*, in addition to thermophilic dinocyst species, corroborates high seasonal gradients of temperatures and warm surface water as

recorded by alkenone and $^{18}O_{G.\ bulloides}$ after the development of the halocline (Haug et al., 2005). During the late Pliocene, a progressive reduction in total pollen grain and spore fluxes, used as tracers of the winds, is recorded at ODP Site 882. This change parallels the southward migration and strengthening of westerly winds, which would have contributed to reinforced moisture supply from low to high latitudes, decreasing the sea-surface salinity in the subarctic Pacific, thus, in turn, acting as a preconditioning mechanism for the initial growth of a regional ice-sheet in northwestern North America. After 1.7 Ma, the dinocyst assemblages at ODP Sites 882 and 887 consist of extant taxa, including *Nematosphaeropsis labyrinthus, Impagidinium pallidum, Operculodinium centrocarpum* and *Brigantedinium* spp., together reflecting subpolar conditions in surface waters across the subarctic Pacific. We attempted to link the replacement of *N. labyrinthus* by *O. centrocarpum* recorded during the last 1.2 Ma, to a progressive increased influence of subtropical waters to the subarctic gyre. Overall, the dinocyst assemblages bring further evidence about the importance of surface ocean conditions in the subpolar North Pacific in modulating the evolution of ice-sheets in the northwestern sector of North America during the Pliocene and the Pleistocene.

Data Availability Statement

The ODP Site 882 palynological data used in the study to reconstruct past oceanic and climate changes during the Plio-Pleistocene are available in the Pangaea Repository (Zorzi & de Vernal, 2024).

Acknowledgments

This study is an ArcTrain contribution. We acknowledge the support provided by the Natural Sciences and Engineering Research Council (NSERC) of Canada through the Collaborative Research and Training Experience (CREATE) program and Discovery Grants to AdV. This study received Portuguese national funds from FCT—Foundation for Science and Technology through projects UIDB/04326/2020 (https://doi.org/10.54499/UIDB/04326/2020), UIDP/04326/2020 (https://doi.org/10.54499/UIDP/04326/2020) and LA/P/0101/2020 (https://doi.org/10.54499/LA/P/0101/2020) and through CZ's contract (https://doi.org/10.54499/2022.03976.CEECIND/CP1729/CT0001). The authors thank the scientific party, technical staff and crews of ODP Leg 145 for their efforts in providing the data and samples used in this research. Finally, the authors would like to express their gratitude to Stijn De Schepper, Vera Pospelova, an anonymous reviewer and Carlos Jaramillo, associated editor, for their careful and perceptive critical comments, which greatly improved the quality of the article.

References

Abell, J. T., Winckler, G., Anderson, R. F., & Herbert, T. D. (2021). Poleward and weakened westerlies during Pliocene warmth. *Nature*, *589*(7840), 70–75. https://doi.org/10.1038/s41586-020-03062-1

Aubry, A. M. R., De Schepper, S., & de Vernal, A. (2020). Dinocyst and acritarch biostratigraphy of the Late Pliocene to Early Pleistocene at Integrated Ocean Drilling Program Site U1307 in the Labrador Sea. *Journal of Micropalaeontology*, *39*(1), 41–60. https://doi.org/10.5194/jm-39-41-2020

Balota, E. J., Head, M. J., Okada, M., Suganuma, Y., & Haneda, Y. (2021). Paleoceanography and dinoflagellate cyst stratigraphy across the Lower–Middle Pleistocene Subseries (Calabrian–Chibanian Stage) boundary at the Chiba composite section, Japan. *Progress in Earth and Planetary Science*, *8*(1), 48. https://doi.org/10.1186/s40645-021-00438-3

Barendregt, R., & Duk-Rodkin, A. (2011). Chronology and extent of Late Cenozoic ice sheets in North America. *Developments in Quaternary Science*, *15*, 419–426. https://doi.org/10.1016/B978-0-444-53447-7.00032-5

Barron, J. A., Basov, I., Beaufort, L., Dubuisson, G., Gladenkov, A. Y., Morley, J. J., et al. (1995). Biostratigraphic and magnetostratigraphic summary. In D. K. Rea, I. A. Basov, D. W. Scholl, & J. F. Allan (Eds.), *Proceedings of the ODP science results* (Vol. 145, pp. 559–575). Ocean Drill. Program. https://doi.org/10.2973/odp.proc.sr.145.145.1995

Barron, J. A., & Gladenkov, A. Y. (1995). Early Miocene to Pleistocene diatom stratigraphy of Leg 145. In D. K. Rea, I. A. Basov, D. W. Scholl, & J. F. Allan (Eds.), *Proceedings of the ODP scientific results* (Vol. 145, pp. 3–19). Ocean Drill. Program. https://doi.org/10.2973/odp.proc.sr.145.101.1995

Bonnet, S., de Vernal, A., Gersonde, R., & Lembke-Jene, L. (2012). Modern distribution of dinocysts from the North Pacific Ocean (37-64°N, 144°E-148°W) in relation to hydrographic conditions, sea-ice and productivity. *Marine Micropaleontology*, *84–85*, 87–113. https://doi.org/10.1594/PANGAEA.807216

Boyer, T. P., Antonov, J. I., Baranova, O. K., Coleman, C., Garcia, H. E., Grodsky, A., et al. (2013). In S. Levitus (Ed.), & A. Mishonov (Technical Ed.), *World Ocean Database (2013)* (Vol. 72, pp. 0–209). NOAA Atlas NESDIS.

Bujak, J. P. (1984). Cenozoic dinoflagellate cysts and acritarchs from the Bering Sea and Northern North Pacific, DSDP Leg 19. *Micropaleontology*, *30*(2), 180–212. https://doi.org/10.2307/1485717

Bujak, J. P., & Matsuoka, K. (1986). Taxonomic reallocation of Cenozoic dinoflagellate cysts from Japan and the Bering Sea. *Palynology*, *10*(1), 235–241. https://doi.org/10.1080/01916122.1986.9989311

Burls, N. J., Fedorov, A. V., Sigman, D. M., Jaccard, S. L., Tiedemann, R., & Haug, G. H. (2017). Active Pacific meridional overturning circulation (PMOC) during the warm Pliocene. *Science Advances*, *3*(9), e1700156. https://doi.org/10.1126/sciadv.1700156

Dale, B. (1996). Dinoflagellate cyst ecology: Modeling and geological applications. In J. Jansonius & D. C. McGregor (Eds.), *Palynology: Principles and applications* (pp. 1249–1276). American Association of Stratigraphic Palynologists Foundation.

De Clercq, J. (2015). *Marine palynomorphs from the Pliocene and Lower Quaternary of the Bering Sea (IODP U1341): A biostratigraphic analysis and paleoenvironmental reconstruction*. Unpublished MSc Thesis (Vol. 116). Universty of Ghent. Retrieved from https://libstore.ugent.be/fulltxt/RUG01/002/213/966/RUG01-002213966_2015_0001_AC.pdf

De Schepper, S. (2006). *Plio-Pleistocene dinoflagellate cyst biostratigraphy and palaeoecology of the eastern North Atlantic and southern North Sea Basin* (PhD Thesis). University of Cambridge.

De Schepper, S., Fischer, E. I., Groeneveld, J., Head, M. J., & Matthiessen, J. (2011). Deciphering the palaeoecology of Late Pliocene and Early Pleistocene dinoflagellate cysts. *Palaeogeography Palaeoclimatology Palaeoecology, Special Issue: Climate and seasonality in a Pliocene warm world*, *309*(1–2), 17–32. https://doi.org/10.1016/j.palaeo.2011.04.020

De Schepper, S., & Head, M. J. (2009). Pliocene and Pleistocene dinoflagellate cyst and acritarch zonation of DSDP Hole 610A, eastern North Atlantic. *Palynology*, *33*(1), 179–218. https://doi.org/10.2113/gspalynol.33.1.179

De Schepper, S., Head, M. J., & Louwye, S. (2004). New dinoflagellate cyst and incertae sedis taxa from the Pliocene of northern Belgium, southern North Sea Basin. *Journal of Paleontology*, *78*(4), 625–644. https://doi.org/10.1666/00223360(2004)078<0625:NDCAIS>2.0.CO;2

De Schepper, S., & McClymont, E. L. (2023). Transition from late Neogene to early Pleistocene environments. *Reference Module in Earth Systems and Environmental Sciences*. https://doi.org/10.1016/B978-0-323-99931-1.00121-5

de Vernal, A., Henry, M., & Bilodeau, G. (1996). Micropaleontological preparation techniques and analyses. *Les Cahiers du Geotop*, *3*, 16–27.

de Vernal, A., Henry, M., Matthiessen, J., Mudie, P. J., Rochon, A., Boessenkool, K. P., et al. (2001). Dinoflagellate cyst assemblages as tracers of sea-surface conditions in the northern North Atlantic, Arctic and sub-Arctic seas: The new 'n = 677' data base and its application for quantitative palaeoceanographic reconstruction. *Quaternary Science Reviews*, *16*(7), 681–698. https://doi.org/10.1002/jqs.659

de Vernal, A., & Pedersen, T. F. (1997). Micropaleontology and palynology of core PAR87A-10: A 23,000 year record of paleoenvironmental changes in the Gulf of Alaska, northeast North Pacific. *Paleoceanography*, *12*(6), 821–830. https://doi.org/10.1029/97PA02167

de Vernal, A., Radi, T., Zaragosi, S., Van Nieuwenhove, N., Rochon, A., Allan, E., et al. (2020). Distribution of common modern dinoflagellate cyst taxa in surface sediments of the Northern Hemisphere in relation to environmental parameters: The new n=1968 database. *Marine Micropaleontology*, *159*, 101796. https://doi.org/10.1016/j.marmicro.2019.101796

Duk-Rodkin, A., Barendregt, R. W., Froese, D. G., Weber, F., Enkin, R., Rod Smith, I., et al. (2004). Timing and extent of Plio-Pleistocene glaciations in north-western Canada and east-Central Alaska. In J. Ehlers & P. L. Gibbard (Eds.), *Developments in Quaternary sciences, Quaternary glaciations-extent and chronology* (pp. 313–345). Elsevier. https://doi.org/10.1016/S1571-0866(04)80206-9

Duprat, L. P. A. M., Bigg, G. R., & Wilton, D. J. (2016). Enhanced Southern Ocean marine productivity due to fertilization by giant icebergs. *Nature Geoscience*, *9*(3), 219–221. https://doi.org/10.1038/ngeo2633

Farmani, T. (2022). *Paleoceanography and dinoflagellate cyst record of northwestern North Pacific ODP Site 882 during the Pliocene–Pleistocene transition* (Unpublished MSc Thesis). Bock University. Retrieved from https://dr.library.brocku.ca/handle/10464/15653?show=full

Favorite, R. (1976). Oceanography of the Subarctic Pacific region, 1960-71. *International North Pacific Fisheries Commission Bulletin*, *33*, 1–187.

Gibbard, P. L., Head, M. J., & Walker, M. J. (2010). The Subcommission on Quaternary Stratigraphy (2010). Formal ratification of the Quaternary System/Period and the Pleistocene Series/Epoch with a base at 2.58 Ma. *Journal of Quaternary Science*, *25*(2), 96–102. https://doi.org/10.1002/jqs.1338

Gray, W. R., Wills, R. C. J., Rae, J. W. B., Burke, A., Ivanovic, R. F., Roberts, W. H. G., et al. (2020). Wind-driven evolution of the North Pacific subpolar Gyre over the last deglaciation. *Geophysical Research Letters*, *47*(6), e2019GL086328. https://doi.org/10.1029/2019GL086328

Haj Soltan, F. (2021). *Paleoceanography across the Pliocene–Pleistocene transition in the southern Bering Sea: Dinoflagellate cysts and acritarchs from IODP Site U1341* (Unpublished MSc Thesis). Bock University. Retrieved from https://dr.library.brocku.ca/handle/10464/15386

Hammer, Ø., Harper, D. A. T., & Ryan, P. D. (2005). PAST: Paleontological statistics software package for education and data analysis.

Haug, G. H., Ganopolski, A., Sigman, D. M., Rosell-Melé, A., Swann, G. E. A., Tiedemann, R., et al. (2005). North Pacific seasonality and the glaciation of North America 2.7 million years ago. *Nature*, *433*(7028), 821–825. https://doi.org/10.1038/nature03332

Haug, G. H., & Sarnthein, M. (2005). Zur Paläo-Ozeanographie und Sedimentationsgeschichte im Nordwest-Pazifik während der letzten 6 Millionen Jahre (ODP-Site 882). https://doi.org/10.1594/PANGAEA.315092

Haug, G. H., Sigman, D. M., Tiedemann, R., Pedersen, T. F., & Sarnthein, M. (1999). Onset of permanent stratification in the subarctic Pacific Ocean. *Nature*, *401*(6755), 779–782. https://doi.org/10.1038/44550

Head, M. J. (1994). Morphology and paleoenvironmental significance of the Cenozoic dinoflagellate genera *Tectatodinium* and *Habibacysta*. *Micropaleontology*, *40*(4), 289–321. https://doi.org/10.2307/1485937

Head, M. J. (1997). Thermophilic dinoflagellate assemblages from the mid Pliocene of eastern England. *Journal of Paleontology*, *71*(2), 165–193. https://doi.org/10.1017/s0022336000039123

Head, M. J. (1998). New goniodomacean dinoflagellates with a compound hypotractal archeopyle from the late Cenozoic: *Capisocysta* Warny and Wrenn, emend. *Journal of Paleontology*, *72*(5), 797–809. https://doi.org/10.1017/S0022336000027153

Head, M. J. (2000). Geonettia waltonensis, a new goniodomacean dinoflagellate fromthe Pliocene of the North Atlantic region, and its evolutionary implications. *Journal of Paleontology*, *74*(5), 812–827. https://doi.org/10.1666/0022-3360(2000)074b0812:GWANGDN2.0.CO;2

Head, M. J., Edwards, L., Garrett, J. K., Lentin, J. K., Marret, F., Matsuoka, K., et al. (1994). A forum on Neogene and Quaternary dinoflagellate cysts: The edited transcript of a round table discussion held at the Third Workshop on Neogene and Quaternary Dinoflagellates; with taxonomic appendix. *Palynology*, *17*(1), 201–239. https://doi.org/10.1080/01916122.1993.9989428

Head, M. J., & Norris, G. (2003). New species of dinoflagellate cysts and other palynomorphs from the latest Miocene and Pliocene of DSDP Hole 603C, western North Atlantic. *Journal of Paleontology*, *77*, 1–15. https://doi.org/10.1666/0022-3360(2003)077b0001:NSODCAN2.0.CO;2

Head, M. J., Norris, G., & Mudie, P. J. (1989). New species of dinocysts and a new species of acritarch from the Upper Miocene and lowermost Pliocene, ODP Leg 105, Site 646, Labrador Sea. In S. P. Srivastava, M. A. Arthur, B. Clement, A. Aksu, J. Baldauf, G. Bohrman, et al. (Eds.), *Proceedings of the ODP scientific results* (Vol. 105, pp. 453–466). Ocean Drill. Program. https://doi.org/10.2973/odp.proc.sr.105.136.1989

Head, M. J., & Wrenn, J. H. (1992). A forum on Neogene and Quaternary dinoflagellate cysts: The edited transcript of a round table discussion held at the Second Workshop on Neogene Dinoflagellates. In M. J. Head & J. H. Wrenn (Eds.), *Neogene and Quaternary Dinoflagellate Cysts and Acritarchs*. American Association of Stratigraphic Palynologists (pp. 1–31).

Hennissen, J. A. I., Head, M. J., De Schepper, S., & Groeneveld, J. (2017). Dinoflagellate cyst paleoecology during the Pliocene–Pleistocene climatic transition in the North Atlantic. *Palaeogeography, Palaeoclimatology, Palaeoecology*, *470*, 81–108. https://doi.org/10.1016/j.palaeo.2016.12.023

Herbert, T. D. (2023). The mid-Pleistocene climate transition. *Annual Review of Earth and Planetary Sciences*, *51*(1), 389–418. https://doi.org/10.1146/annurev-earth-032320-104209

Honda, M. C., Kawakami, H., Sasaoka, K., Watanabe, S., & Dickey, T. (2006). Quick transport of primary produced organic carbon to the ocean interior. *Geophysical Research Letters*, *33*(16). https://doi.org/10.1029/2006GL026466

Horikawa, K., Martin, E. E., Basak, C., Onodera, J., Seki, O., Sakamoto, T., et al. (2015). Pliocene cooling enhanced by flow of low-salinity Bering Sea water to the Arctic Ocean. *Nature Communications*, *6*(1), 7587. https://doi.org/10.1038/ncomms8587

Juggins, S. (2020). rioja: Analysis of quaternary science data. *R package version 0.9-26*. Retrieved from https://cran.r-project.org/package=rioja

Kamikuri, S., Nishi, H., & Motoyama, I. (2007). Effects of late Neogene climatic cooling on North Pacific radiolarian assemblages and oceanographic conditions. *Palaeogeography, Palaeoclimatology, Palaeoecology*, *249*(3–4), 370–392. https://doi.org/10.1016/j.palaeo.2007.02.008

Kanazawa, T., Sager, W. W., Escutia, C., Araki, E., Arney, J. E., Carlson, R. L., et al. (2001). *Proceedings of the ODP, initial reports* (Vol. 191). Ocean Drilling Program. https://doi.org/10.2973/odp.proc.ir.191.2001

Kender, S., Ravelo, A. C., Worne, S., Swann, G. E. A., Leng, M. J., Asahi, H., et al. (2018). Closure of the Bering Strait caused mid-Pleistocene transition cooling. *Nature Communications*, *9*(1), 5386. https://doi.org/10.1038/s41467-018-07828-0

Kurita, H., & Obuse, A. (2003). Dinoflagellate cyst biostratigraphy of ODP Hole 186-1151A sediments. Suppl. Kurita, H., Obuse, a., 2003 Middle Miocene-Uppermost Lower Pliocene dinoflagellate cyst biostratigraphy ODP Leg 186 Hole 1151A Sanriku Coast North Japan Northwest

Pacific. In K. Suyehiro, I. S. Sacks, G. D. Acton, & M. Oda (Eds.), *Proceedings of the ODP, scientific results* (Vol. 186, pp. 1–19). Ocean Drilling Program. https://doi.org/10.1594/PANGAEA.783436

Lagoe, M. B., & Zellers, S. D. (1996). Depositional and microfaunal response to Pliocene climate change and tectonics in the eastern Gulf of Alaska. *Marine Micropaleontology, Climates and Climate Variability of the Pliocene*, *27*(1–4), 121–140. https://doi.org/10.1016/0377-8398(95)00055-0

Lam, P. J., & Bishop, J. K. (2008). The continental margin is a key source of iron to the HNLC North Pacific Ocean. *Geophysical Research Letters*, *35*(7). https://doi.org/10.1029/2008GL033294

LaRiviere, J. P., Ravelo, A. C., Crimmins, A., Dekens, P. S., Ford, H. L., Lyle, M., & Wara, M. W. (2012). Late Miocene decoupling of oceanic warmth and atmospheric carbon dioxide forcing. *Nature*, *486*(7401), 97–100. https://doi.org/10.1038/nature11200

Limoges, A., Van Nieuwenhove, N., Head, M. J., Mertens, K. N., Pospelova, V., & Rochon, A. (2020). A review of rare and less well known extant marine organic-walled dinoflagellate cyst taxa of the orders Gonyaulacales and Suessiales from the Northern Hemisphere. *Marine Micropaleontology*, *159*, 101801. https://doi.org/10.1016/j.marmicro.2019.101801

Lisiecki, L. E., & Raymo, M. E. (2005). A Pliocene-Pleistocene stack of 57 globally distributed benthic d18O records. *Paleoceanography*, *20*(1), PA1003. https://doi.org/10.1029/2004PA001071

Mahowald, N. M., Baker, A. R., Bergametti, N., Brooks, R. A., Duce, T. D., Jickells, N., et al. (2005). Atmospheric global dust cycle and iron inputs to the ocean. *Global Biogeochemical Cycles*, *19*(4), GB4025. https://doi.org/10.1029/2004GB002402

Marret, F., de Vernal, A., Pedersen, T. F., & McDonald, D. (2001). Middle Pleistocene to Holocene palynostratigraphy of Ocean Drilling Program Site 887 in the Gulf of Alaska, northeastern northeastern North Pacific. *Canadian Journal of Earth Sciences*, *38*(3), 373–386. https://doi.org/10.1139/e00-092

Maslin, M. A., Li, X. S., Loutre, M. F., & Berger, A. (1998). The contribution of orbital forcing to the progressive intensification of Northern Hemisphere glaciation. *Quaternary Science Reviews*, *17*(4–5), 411–426. https://doi.org/10.1016/S0277-3791(97)00047-4

Matsuoka, K. (1983). Late Cenozoic dinoflagellates and acritarchs in the Niigata District, Central Japan. *Palaeontographica Abteilung B*, *187*, 89–154.

Matsuoka, K., & Bujak, J. P. (1988). Cenozoic dinoflagellate cysts from the Navarin Basin, Norton Sound and St. George Basin, Bering Sea. *Bulletin of the Faculty of Liberal Arts, Nagasaki University, Natural Science*, *29*, 1–147.

Matsuoka, K., Bujak, J. P., & Shimazaki, T. (1987). Late Cenozoic dinoflagellate cyst biostratigraphy from the west coast of Northern Japan. *Micropaleontology*, *33*(3), 214–229. https://doi.org/10.2307/1485638

Matsuzaki, K. M., Suzuki, N., Nishi, H., Hayashi, H., Gyawali, B. R., Takashima, R., & Ikehara, M. (2015). Early to Middle Pleistocene paleoceanographic history of southern Japan based on radiolarian data from IODP Exp. 314/315 Sites C0001 and C0002. *Marine Micropaleontology*, *118*, 17–33. https://doi.org/10.1016/j.marmicro.2015.05.001

Matthews, J. (1969). The assessment of a method for the determination of absolute pollen frequencies. *New Phytologist*, *68*(1), 161–166. https://doi.org/10.1111/j.1469-8137.1969.tb06429.x

Matthiessen, J., & Brenner, W. (1996). Dinoflagellate cyst ecostratigraphy of Pliocene-Pleistocene sediments from the Yermak Plateau (Arctic Ocean, Hole 911A). In *Proceedings of the ODP, scientific results* (Vol. 151, pp. 243–253). Ocean Drilling Program. https://doi.org/10.2973/odp.proc.sr.151.109.1996

Matthiessen, J., Schreck, M., De Schepper, S., Zorzi, C., & de Vernal, A. (2018). Quaternary dinoflagellate cysts in the Arctic Ocean: Potential and limitations for stratigraphy and paleoenvironmental reconstructions. *Quaternary Science Reviews*, *192*, 1–26. https://doi.org/10.1016/j.quascirev.2017.12.020

Meire, L., Meire, P., Struyf, E., Krawczyk, D. W., Arendt, K. E., Yde, J. C., et al. (2016). High export of dissolved silica from the Greenland Ice Sheet. *Geophysical Research Letters*, *43*(17), 9173–9182. https://doi.org/10.1002/2016GL070191

Mertens, K. N., Verhoeven, K., Verleye, T., Louwye, S., Amorim, A., Ribeiro, S., et al. (2009). Determining the absolute abundance of dinoflagellate cysts in recent marine sediments: The *Lycopodium* marker-grain method put to the test. *Review of Palaeobotany and Palynology*, *157*(3–4), 238–252. https://doi.org/10.1016/j.revpalbo.2009.05.004

Meyers, S. R. (2019). Cyclostratigraphy and the problem of astrochronologic testing. *Earth-Science Reviews*, *190*, 190–223. https://doi.org/10.1016/j.earscirev.2018.11.015

Morley, J. J., & Nigrini, C. (1995). Miocene to Pleistocene radiolarian biostratigraphy of North Pacific Sites 881,884,885,886, and 887. In D. K. Rea, I. A. Basov, D. W. Scholl, & J. F. Allan (Eds.), *Proceedings of the ODP scientific results* (Vol. 145, pp. 55–91). Ocean Drill. Program. https://doi.org/10.2973/odp.proc.sr.145.107.1995

Mudelsee, M., & Stattegger, K. (1997). Exploring the structure of the mid-Pleistocene revolution with advanced methods of time-series analysis. *Geologische Rundschau*, *86*(2), 499–511. https://doi.org/10.1007/s005310050157

Müller, J., Romero, O., Cowan, E. A., McClymont, E. L., Forwick, M., Asahi, H., et al. (2018). Cordilleran ice-sheet growth fueled primary productivity in the Gulf of Alaska, northeast Pacific Ocean. *Geology*, *46*(4), 307–310. https://doi.org/10.1130/G39904.1

Murphy, M. A., & Salvador, A. (1999). International stratigraphic guide — An abridged version. *Episodes Journal of International Geoscience*, *22*(4), 255–271. https://doi.org/10.18814/epiiugs/1999/v22i4/002

Nishioka, J., Takeda, S., Kudo, I., Tsumune, D., Yoshimura, T., Kuma, K., & Tsuda, A. (2003). Size-fractionated iron distributions and iron-limitation processes in the subarctic NW Pacific. *Geophysical Research Letters*, *30*(14). https://doi.org/10.1029/2002GL016853

Ogg, J. G. (2012). Chapter 5 – Geomagnetic polarity time scale. In F. M. Gradstein, J. O. Ogg, M. D. Schmitz, & G. M. Ogg (Eds.), *The geologic time scale* (pp. 85–113). https://doi.org/10.1016/B978-0-444-59425-9.00005-6

Penaud, A., Eynaud, F., Turon, J. L., Zaragosi, S., Marret, F., & Bourillet, J. F. (2008). Interglacial variability (MIS 5 and MIS 7) and dinoflagellate cyst assemblages in the Bay of Biscay (North Atlantic). *Marine Micropaleontology*, *68*(1–2), 136–155. https://doi.org/10.1016/j.marmicro.2008.01.007

Pisias, N. G., & Moore, T. C. (1981). The evolution of Pleistocene climate: A time series approach. *Earth and Planetary Science Letters*, *52*(2), 450–458. https://doi.org/10.1016/0012-821X(81)90197-7

Pospelova, V., de Vernal, A., & Pedersen, T. F. (2008). Distribution of dinoflagellate cysts in surface sediments from the northeastern Pacific Ocean (43–25°N) in relation to sea-surface temperature, salinity, productivity and coastal upwelling. *Marine Micropaleontology*, *68*(1–2), 21–48. https://doi.org/10.1016/j.marmicro.2008.01.008

Qiu, B. (2000). Interannual variability of the Kuroshio Extension system and its impact on the wintertime SST field. *Journal of Physical Oceanography*, *30*(6), 1486–1502. https://doi.org/10.1175/1520-0485(2000)030<1486:IVOTKE>2.0.CO;2

Radi, T., & de Vernal, A. (2004). Dinocyst distribution in surface sediments from the northeastern Pacific margin (40–60 N) in relation to hydrographic conditions, productivity and upwelling. *Review of Palaeobotany and Palynology*, *128*(1–2), 169–193. https://doi.org/10.1016/S0034-6667(03)00118-0

Radi, T., & de Vernal, A. (2008). Dinocysts as proxy of primary productivity in mid–high latitudes of the Northern Hemisphere. *Marine Micropaleontology*, *68*(1–2), 84–114. https://doi.org/10.1016/j.marmicro.2008.01.012

R Core Team. (2021). *R: A language and environment for statistical computing*. R Foundation for Statistical Computing. Retrieved from https://www.R-project.org/

Rea, D. K., Basov, I. A., Scholl, D. W., & Allan, J. F. (1995). *Proceedings of the ODP, scientific results* (Vol. 145). Ocean Drilling Program. https://doi.org/10.2973/odp.proc.sr.145.1995

Rea, D. K., & Snoeckx, H. (1995). Sediment fluxes in the Gulf of Alaska: Paleoceanographic record from site 887 on the Patton-Murray seamount platform. In D. K. Rea, I. A. Basov, D. W. Scholl, & J. F. Allan (Eds.), *Proceedings of the ODP, scientific results* (Vol. 145, pp. 247–256). Ocean Drilling Program. https://doi.org/10.2973/odp.proc.sr.145.122.1995

Reece, R. S., Gulick, S. P. S., Horton, B. K., Christeson, G. L., & Worthington, L. L. (2011). Tectonic and climatic influence on the evolution of the Surveyor Fan and Channel system, Gulf of Alaska. *Geosphere*, *7*(4), 830–844. https://doi.org/10.1130/GES00654.1

Rochon, A., de Vernal, A., Turon, J.-L., Matthiessen, J., & Head, M. J. (1999). Distribution of recent dinoflagellate cysts in surface sediments from the North Atlantic Ocean and adjacent seas in relation to sea-surface parameters. *American Association of Stratigraphic Palynologists Contributions Series*, *35*, 1–146.

Sánchez-Montes, M. L., McClymont, E. L., Lloyd, J. M., Müller, J., Cowan, E. A., & Zorzi, C. (2020). Late Pliocene Cordilleran Ice Sheet development with warm northeast Pacific sea surface temperatures. *Climate of the Past*, *16*(1), 299–313. https://doi.org/10.5194/cp-16-299-2020

Sánchez-Montes, M. L., Romero, O. E., Cowan, E. A., Müller, J., Moy, C. M., Lloyd, J. M., & McClymont, E. L. (2022). Plio-Pleistocene ocean circulation changes in the Gulf of Alaska and its impacts on the carbon and nitrogen cycles and the Cordilleran ice sheet development. *Paleoceanography and Paleoclimatology*, *37*(7), e2021PA004341. https://doi.org/10.1029/2021PA004341

Schlitzer, R. (2016). Ocean data View. Retrieved from http://odv.awi.de

Schreck, M., Nam, S.-I., Clotten, C., Fahl, K., De Schepper, S., Forwick, M., & Matthiessen, J. (2017). Neogene dinoflagellate cysts and acritarchs from the high northern latitudes and their relation to sea surface temperature. *Marine Micropaleontology*, *136*, 51–65. https://doi.org/10.1016/j.marmicro.2017.09.003

Shimada, C., Sato, T., Yamasaki, M., Hasegawa, S., & Tanaka, Y. (2009). Drastic change in the late Pliocene subarctic Pacific diatom community associated with the onset of the Northern Hemisphere Glaciation. *Palaeogeography, Palaeoclimatology, Palaeoecology*, *279*(3–4), 207–215. https://doi.org/10.1016/j.palaeo.2009.05.015

Sigman, D. M., Jaccard, S. L., & Haug, G. H. (2004). Polar ocean stratification in a cold climate. *Nature*, *428*(6978), 59–63. https://doi.org/10.1038/nature02357

Stroynowski, Z., Ravelo, A. C., & Andreasen, D. (2015). A Pliocene to recent history of the Bering Sea at Site U1340A, IODP Expedition 323. *Paleoceanography*, *30*(12), 1641–1656. https://doi.org/10.1002/2015PA002866

Taylor, S. P., Patterson, M. O., Lam, A. R., Jones, H., Woodard, S. C., Habicht, M. H., et al. (2022). Expanded North Pacific subtropical Gyre and Heterodyne expression during the mid-Pleistocene. *Paleoceanography and Paleoclimatology*, *37*(5), e2021PA004395. https://doi.org/10.1029/2021PA004395

Tiedemann, R., & Haug, G. H. (1995). Astronomical calibration of cycle stratigraphy for Site 882 in the northwest Pacific. In D. K. Rea, I. A. Basov, D. W. Scholl, & J. F. Allan (Eds.), *Proceedings of the ODP scientific results* (Vol. 145, pp. 3–19). Ocean Drill. Program. https://doi.org/10.2973/odp.proc.sr.145.124.1995

Van Nieuwenhove, N., Head, M. J., Limoges, A., Pospelova, V., Mertens, K. N., Matthiessen, J., et al. (2020). An overview and brief description of common marine organic-walled dinoflagellate cyst taxa occurring in surface sediments of the Northern Hemisphere. *Marine Micropaleontology*, *159*, 101814. https://doi.org/10.1016/j.marmicro.2019.101814

Verhoeven, K., & Louwye, S. (2013). Palaeoenvironmental reconstruction and biostratigraphy with marine palynomorphs of the Plio–Pleistocene in Tjörnes, Northern Iceland. *Palaeogeography, Palaeoclimatology, Palaeoecology*, *376*, 224–243. https://doi.org/10.1016/j.palaeo.2013.03.002

Warren, B. A. (1983). Why is no deep water formed in the North Pacific? *Journal of Marine Research*, *41*(2), 327–347. https://doi.org/10.1357/002224083788520207

Weeks, R. J., Roberts, A. P., Verosub, K. L., Okada, M., & Dubuisson, G. J. (1995). Magnetostratigraphy of upper Cenozoic sediments from Leg 145, North Pacific Ocean. In D. K. Rea, I. A. Basov, D. W. Scholl, & J. F. Allan (Eds.), *Proceedings of the ODP scientific results* (Vol. 145, pp. 491–521). Ocean Drill. Program. https://doi.org/10.2973/odp.proc.sr.145.138.1995

Yuan, X., & Talley, L. D. (1996). The subarctic frontal zone in the North Pacific: Characteristics of frontal structure from climatological data and synoptic surveys. *Journal of Geophysical Research*, *101*(C7), 16491–16508. https://doi.org/10.1029/96JC01249

Zonneveld, K. A., Versteegh, G., & Kodrans-Nsiah, M. (2008). Preservation and organic chemistry of Late Cenozoic organic-walled dinoflagellate cysts: A review. *Marine Micropaleontology*, *68*(1–2), 179–197. https://doi.org/10.1016/j.marmicro.2008.01.015

Zonneveld, K. A. F., Bockelmann, F., & Holzwarth, U. (2007). Selective preservation of organic-walled dinoflagellate cysts as a tool to quantify past net primary production and bottom water oxygen concentrations. *Marine Geology*, *237*(3–4), 109–126. https://doi.org/10.1016/j.margeo.2006.10.023

Zonneveld, K. A. F., Marret, F., Versteegh, G. J. M., Bogus, K., Bonnet, S., Bouimetarhan, I., et al. (2013). Atlas of modern dinoflagellate cyst distribution based on 2405 data points. *Review of Palaeobotany and Palynology*, *191*, 1–197. https://doi.org/10.1016/j.revpalbo.2012.08.003

Zonneveld, K. A. F., Versteegh, G. J. M., & de Lange, G. J. (1997). Preservation of organic-walled dinoflagellate cysts in different oxygen regimes: A 10,000 year natural experiment. *Marine Micropaleontology*, *29*(3–4), 393–405. https://doi.org/10.1016/S0377-8398(96)00032-1

Zorzi, C., & de Vernal, A. (2024). Palynological dataset at ODP Site 882 (North Pacific) during the Plio-Pleistocene [dataset]. *PANGAEA*. https://doi.org/10.1594/PANGAEA.969032

Zorzi, C., Head, M. J., Matthiessen, J., & de Vernal, A. (2019). *Impagidinium detroitense* and *I.*? *diaphanum*: Two new dinoflagellate cyst species from the Pliocene of the North Pacific Ocean, and their biostratigraphic significance. *Review of Palaeobotany and Palynology*, *264*, 24–37. https://doi.org/10.1016/j.revpalbo.2019.02.005

Zorzi, C., Matthiessen, J., & de Vernal, A. (2020). Palynology, biostratigraphy, and paleoceanography of the Plio-Pleistocene at Ocean Drilling Program Site 887, Gulf of Alaska. *Palaeogeography, Palaeoclimatology, Palaeoecology*, *546*, 109605. https://doi.org/10.1016/j.palaeo.2020.109605